Manufacturing and physico-mechanical characterization of carbon nanohorns/polyacrylonitrile nanocomposites

Aneta Fraczek-Szczypta · Stanislaw Blazewicz

Abstract The use of carbon nanohorns (SWCNHs) as a modifying filler in a polyacrylonitrile (PAN) matrix is studied with the goal of elaborating nanocomposites. The study deals with assessment of the dispersity of SWCNHs in a PAN polymer suspension. The SWCNHs were introduced into the PAN-based suspension using different methods, including mechanical stirring, ultrasonification and the combination of ultrasonification with addition of a surfactant. Agglomeration and dispersion processes of SWCNH in the polymer suspensions were studied using DLS technique and turbidimetry. The resulting properties of nanocomposite foils after solidification in water ambient were verified in various tests. The mechanical tensile properties (tensile strength, modulus and strain to fracture) of the nanocomposites before and after the dispersion process were compared. The nanocomposites obtained under optimally prepared suspension perform the highest strain to fracture in tensile test. Electrical resistivity and thermal conductivity of nanocomposites samples after appropriate dispersion of SWCNHs in the PAN suspension were also determined. The presence of SWCNH in the PAN suspension affects the structure of nanocomposites after solidification through changing structural ordering of the polymer. The study revealed that the polymeric suspensions prepared in optimum processing conditions contain the carbon aggregates the size of which correspond almost to the mean size of a *dahlia flower-like* structured particle, i.e., 50–250 nm and it was not possible to separate such particles into a single form of carbon nanohorn by the techniques used.

Introduction

Single walled carbon nanohorns (SWCNHs) constitute a potential nanoconstituent for manufacture of polymer-based nanocomposites [1, 2]. Individual SWCNHs have an unique structural feature represented by a typical diameter of 2 nm with a length of 30–50 nm. The end of this tube is closed by a conical cap with a cone angle of 20°. These individual SWCNHs (CNHs) have a tendency to couple together and form a stable *dahlia flower-like* structured particle with a narrow diameter distribution of 80–100 nm [3, 4]. SWCNHs belong to the carbon nanotube family [1, 4], not yet available commercially [4]. The SWCNH particle due to a high surface energy creates bigger aggregates in its as-received form. Such nanoparticles, like other tubular forms of carbon nanotubes can be easily chemically modified and are good electrical conductors. Their high energy adsorption is especially attractive for fuel cell technology and gas storage devices. Due to their specific spherical shape of sub-micron diameter they are expected to have attractive tribological and thermal properties [5, 6]. Different nanotubes are nowadays commonly used in nanocomposite technology. The incorporation of such nanoparticles in certain polymeric matrices distinctly affects their physical and mechanical behaviours.

Polyacrylonitrile represents a wide range of polymeric materials (homopolymers, copolymers) available for use in technical and medical applications. It is a thermoplastic polymer with a relative high melting point, high thermal stability and interesting mechanical properties. The PAN-based copolymers are widely used as fibres for textile

A. Fraczek-Szczypta · S. Blazewicz (✉)
Faculty of Materials Science and Ceramics, Department of Biomaterials, AGH-University of Science and Technology in Krakow, al.Mickiewicza 30, 30-059 Krakow, Poland
e-mail: blazew@agh.edu.pl

industry and producing fibrous precursors for carbon fibres [7–9]. The PAN polymer has also been used in separation membrane materials and porous membranes for lithium-ion polymer batteries [10, 11]. The combination of the polyacrylonitrile matrix with carbon nanohorns with their spherical shape creates a new application potential in comparison with more popular carbon nano-tubes [12–15]. The high surface area of SWCNH ranged from 330 to 1300 m²/g and its greater interhorn-wall distance (0.4 nm) than the interlayer spacing of graphite (0.335 nm) have a particular interest for electrochemical purposes [16–18]. Its wider application for the production of new composites is hindered by an agglomeration phenomenon [19–21]. The agglomerates in the PAN matrices and especially in the PAN-based carbon matrix (PAN precursor) impair physicochemical properties of the resulting composites [22].

A great effort has been made to develop various physical and chemical methods of surface modifications of CNTs/CNHs and application of suitable solvents and surfactants reducing the surface tension of polymeric suspensions containing such nanofillers [23–29].

Our earlier studies showed that the addition of single- or multi-wall carbon nanotubes to a PAN solution may lead to altering rheological properties and crystallinity of the polymer matrix after solidification [30, 31]. Mechanical properties of the resulting nanocomposites are dependent upon surface chemical state of carbon nanofillers and their uniform dispersion in a polymer matrix.

Despite many scientific researches dealing with the PAN-based nanocomposites modified with carbon nanofillers, carbon nanohorns-based polymer nanocomposites are not widely reviewed in the literature.

This study compares efficiency of different procedures of preparation of SWCNHs—contained PAN suspensions to achieve minimum value of carbon aggregates. We assumed that the minimum value of SWCNHs correspond to their *dahlia flower-like* structure. The prepared in different way suspensions were used to manufacture the nanocomposite films and their selected properties were determined. Dispersion process of SWCNHs in the polymer solution was controlled by the dynamic light scattering method and radiation absorption.

Materials and method

The SWCNHs were made by the arc discharge process (provided by NanoCraft, Inc. of Renton, USA). They had diameters in the range of 2–3 nm and were 30–50 nm long with a 19° closed-end called a carbon nanohorn. The TEM study of this as-fabricated carbon material revealed that the *dahlia flower-like* carbon domains ranged from 30 to 120 nm (Fig. 1a, b). They were grown in the presence of iron as a catalyst. The iron concentration determined by atomic absorption spectrometry using the electro thermal technique (spectrometer Model 3110, Perkin-Elmer Co.) was about 1.8 wt%.

The three-component PAN polymer matrix consisted of 93–94 wt% of acrylonitrile, 5–6 wt% of methyl acrylate mer units and 1 wt% sodium alilosulfonate (produced by Zoltek Co., Nyegesujtalu, Hungary) was used to manufacture the nanocomposite samples. The samples with SWCNHs have been prepared in the form of thin films and plates.

The following procedures for preparation of the SWCNHs/PAN suspensions were used:

I.   Carbon nanohorns (0.5 wt% SWCNH) were directly introduced into the 10% PAN solution and sonicated at room temperature for 60 min using an ultrasonic homogenizer (MS). PALMER INSTRUMENTS, (Model: CP 130 PB, 130 W power, 20 kHz)
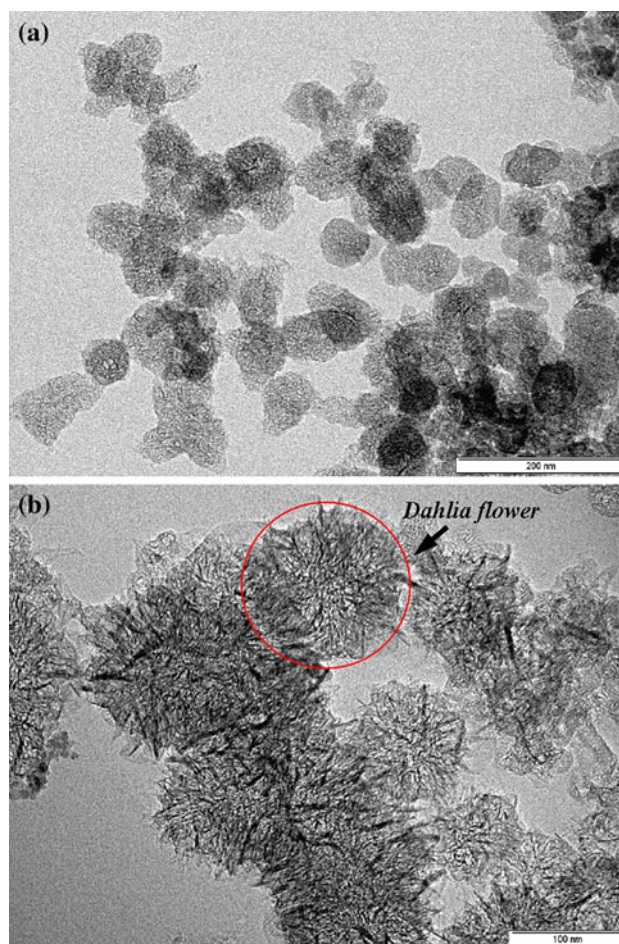

Fig. 1 TEM microphotograph of SWCNH. **a** The product consisted of nearly uniform sized spherical particles (*dahlia flower-like* structure). **b** Higher magnified TEM microphotograph of SWCNH

II. Carbon nanohorns (0.5 wt% SWCNH) were immersed in the dimethylformamide (DMF) solvent, sonicated at room temperature for 60 min with the ultrasonic homogenizer (SD), and subsequently the PAN polymer was added to the DMF/SWCNTHs solution and stirred until the polymer was dissolved (SU).

III. Carbon nanohorns (0.5 wt% SWCNHs) were immersed in DMF, sonicated at room temperature for 60 min with the ultrasonic homogenizer (SD) then PAN was added to the DMF/SWCNH solution (10% PAN solution) and sonicated at room temperature for 30 min (SU10).

The ranges of experimental processing variables (PAN-based solution concentration, amount of nanohorns in suspension, ultrasounds frequency and power, sonication time) have been selected on the basis of our earlier experiences [30, 32–34]. The ultrasound power output and sonication time were chosen adequately to the sample volume. The sonication process was performed under a constant ultrasound power of 20 W. A higher ultrasound power output generated a temperature increase of the polymer suspension. To avoid the possible polymer degradation all experiments were realized under a constant ultrasound power. The lowest limit of nanohorns content being 0.5 wt% was also selected taking into account our earlier experiments [13, 35].

Using the third procedure, two additional suspensions differing in the amount of SWCNH (1 and 3 wt%) were prepared. In our experiments the surfactant Triton®X-100, (POCH Co.) was chosen to reduce the surface tension of the PAN suspensions. It is a non-ionic surfactant consisting of a hydrophilic polyethylene oxide and a hydrocarbon lipophilic or hydrophobic group and is one of the most popular surfactants for dispersion of carbon nanomaterials in organic, water and polymer matrices [26, 36, 37].

The prepared in such a way suspensions were then poured onto the petri dish and left to evaporate the solvent at 40 °C. The nanocomposite films of 60 μm thickness were formed.

Six types of samples based on the PAN solution containing SWCNHs were manufactured. Their description and denotation used this study are gathered in Table 1.

The morphology of SWCNHs was analysed using transmission electron microscopy (TEM) [Tecnai G2 F20 (200 kV)]. Particles size (agglomerates) was carried out in the PAN polymer solutions using DLS technique (Dynamic Light Scattering, Malvern Zetasizer Nano ZS) in the range from 0.6 nm to 6 μm, with the laser light source of wavelength $\lambda = 520$ nm. The degree of dispersion of SWCNHs in the PAN solution was also determined by means of turbidimetry (Hach Model 2100AN IS). This method depends upon absorption measurement of the near-infrared radiation by carbon nanotubes. Light-emitting

Table 1 Description of samples used in this study

Samples	Description
PAN	The control PAN film obtained from 10% PAN solution in DMF
MS	SWCNH/PAN composite film; (0.5% carbon nanohorns in 10% PAN solution) suspension sonicated in the PAN solution only
SU10	SWCNH/PAN composite film (0.5% carbon nanohorns in 10% PAN solution)—gradual sonication, first in DMF and then in the PAN solution
SU10t	SWCNH/PAN composite film (0.5% carbon nanohorns in 10% PAN solution)—gradual sonication in DMF with 1% surfactant and then in the PAN solution
SU10a	SWCNH/PAN composite film (1% carbon nanohorns in 10% PAN solution)—gradual sonication in DMF and then in the PAN solution
SU10b	SWCNH/PAN composite film (3% carbon nanohorns in 10% PAN solution)—gradual sonication in DMF and then in the PAN solution
SU10at	SWCNH/PAN composite film (1% carbon nanohorns in 10% PAN solution)—gradual sonication in DMF with 1% surfactant and then in PAN solution

diode (LED) of the wavelength $\lambda = 870 \pm 30$ nm was the radiation source.

The tensile mechanical tests of the nanocomposites were made using the samples with dimensions of $5 \times 40 \times 0.06$ mm. The tensile strength, modulus and strain to fracture were determined on an universal testing machine Zwick model 1435, PC controlled by TestXpert v.8.1 software Germany, with the crosshead speed of 2 mm/min. The tensile modulus was determined from the slope of initial linear part of the force–strain function. The quantitative results were presented as mean ± standard error of mean (SEM) calculated from five individual measurements. Measuring the changes in the mechanical properties of the nanocomposites is a particularly useful method for the evaluation of effectiveness of the dispersion process.

Microstructural parameters of the pure PAN and nanocomposites were determined from X-ray diffraction (Philips system, $k = 1.54$ Å) using the Scherrer equation.

Differential Scanning Calorimetry (DSC) (NETZSCH STA 449 F3 Jupiter®) was used to determine the differences between the pure PAN samples and PAN-based nanocomposites containing SWCNHs. The weighed amount of the samples (9 mg) was placed in an alumina crucible and heated in nitrogen atmosphere at 10 °C/min heating rate to 600 °C.

Electrical resistivity was measured on the samples made in the form of films ($15 \times 35 \times 0.06$ mm) using a current–voltage two-point probe by means of a digital multimeter (Metex M-3610). An average value of resistivity was calculated from ten individual measurements.

The cut-bar (comparative) method was applied to carry out thermal conductivity coefficient. For this method the samples in the form of plates were specially manufactured by compression moulding. The samples were formed by placing several thin nanocomposite thin films 0.06 mm thick in a metallic mould followed by its slow heating. The filled mould was exposed to compression under a constant pressure of 1.5 MPa at 260 °C. The pressure and temperature were maintained for the determined time followed by cooling the set-up below 100 °C before releasing the pressure and removing the samples from the mould. In such a way the samples in the form of flat plates had the dimensions of 15 × 30.5 × 1.5 mm.

The coefficient of thermal conductivity was determined in steady-state thermal conditions. In this technique, a test system consisted of two plates of a standard material of determined conductivity and the studied (nanocomposite) sample. The nanocomposite was placed between two standards. The measurements were made in the temperature range below 100 °C.

Results and discussion

The Fig. 2 compares the agglomerate size distributions of carbon nanoparticles in the PAN suspensions prepared in three different ways. The suspensions contained the same concentration of nanohorns and were sonicated with ultrasounds for 60 min. The single cluster diameters formed by carbon nanohorns ranged from 30 to 120 nm (Fig. 1a, b), whilst the carbon aggregates (as-prepared nanohorn particles) determined in the PAN suspension before dispersion vary from 1281 to 6439 nm.

It is evident from Fig. 2 that the sizes of aggregated nanohorns and their distributions are dependent upon the procedure of the suspension preparation. Mean size of the agglomerates in the DMF suspension subjected to sonication followed by the PAN suspension preparation is about

142 nm (SU10). On the contrary, an introduction of the aggregated carbon nanohorns directly to the PAN solution and sonication causes formation of the secondary agglomerates of 3091 nm large (MS). In the instance when the dispersion was realized using a gradual sonication in DMF and subsequent stirring in the PAN solution (SU), a bimodal distribution of carbon nanohorns was observed (mean values: 255 and 5560 nm, respectively). These three procedures of preparation of SWCNHs-containing PAN suspensions reveal a strong influence of the sonication phase, i.e., a gradual sonication of the suspension with nanohorns, first in DMF and subsequently in 10% PAN solution which leads to distinctly stronger dispersion of nanohorns. The third procedure of dispersion of carbon nanohorns in polymer solution seems to be the most effective one. The size distribution of SWCNHs in the PAN polymer is very similar to that of SWCNHs in pure DMF (SD) (Fig. 3). These results confirm the favourable influence of a gradual sonication on the disintegration of carbon aggregates in the polymer suspension. On the contrary, an addition of the PAN polymer to the DMF suspension augments solution viscosity, which favours secondary carbon agglomerating.

The effect of a nonionic surfactant on dispersion of SWCNHs in the PAN solution using 1 wt% Triton®X-100 is illustrated in Fig. 4. The preparation of SWCNHs with this surfactant and polymer solution (SU10t) was identical like for the SU10 sample. The figure demonstrates the agglomerate size distribution of SWCNHs in both solutions.

The results show that the presence of surfactant in the polymer suspension enhances dispersion of the aggregated carbon nanohorns. The mean size of agglomerates for this sample (SU10t) found to be 91 nm is lower as compared to the samples without the surfactant (SU10), i.e., 142 nm. The agglomerates formed in the SU10 and in SU10t suspensions varied from 70 to 295 nm and from 50 to 250 nm, respectively. It is worth to note that the size range of the
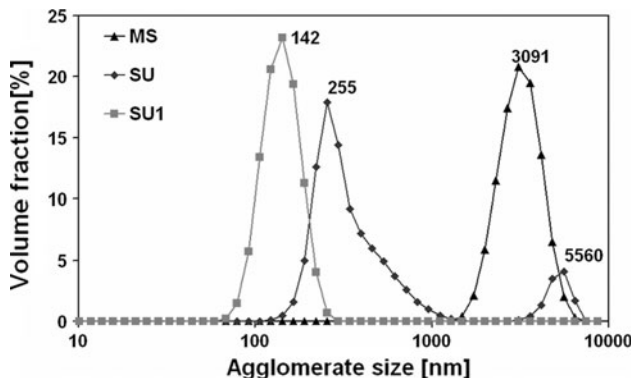

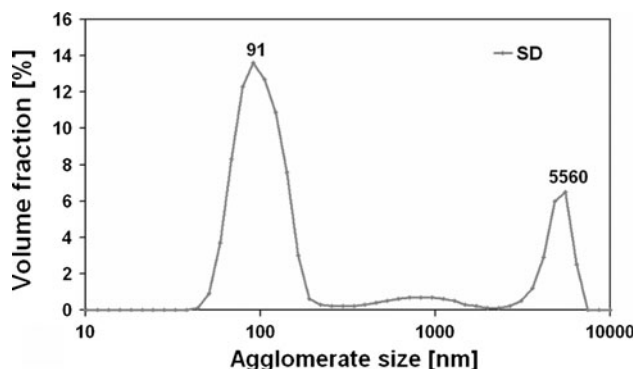**Fig. 2** Agglomerate size distribution of single wall carbon nanohorns in PAN solutions

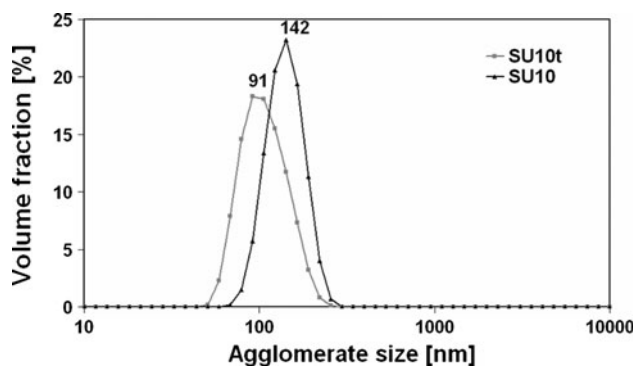**Fig. 3** Size distribution of single wall carbon nanohorns in pure DMF solution

Fig. 4 Agglomerate size distribution of single wall carbon nanohorns in PAN solutions with addition of Triton®X-100

dahlia flower domains of nanohorns (30–120 nm) overlaps in part the ranges of carbon aggregate dimensions found in both suspensions (SU10 and SU10t).

The pure PAN solution and PAN solution containing carbon nanohorns after optimal dispersion (SU10) are shown in Fig. 5. The figure confirms homogenous distribution of nanoparticles in the PAN polymer solution.

Carbon aggregate disintegration process in polymer suspensions was also studied by measuring the absorbance of infrared radiation. Carbon nanohorns in a polymer suspension constitute an absorbent for the near-infrared radiation. Due to the electronic band structure [38–42] the energy gap in carbon nanohorns corresponds to radiation energy for visible and the near-infrared spectra. A suspension with a better dispersion of SWCNHs absorbs IR stronger than a suspension with poorly distributed nanoparticles. The total absorbances measured for carbon nanohorns in the PAN solutions are gathered in Fig. 6.

The diagram shows a different level of absorbance depending on the procedure of preparation of the polymer suspensions. The results confirm that application of gradual sonication of SWCNH, first in DMF and consecutive in the PAN solution (SU10) with surfactant (SU10t) allows for an effective dispersion of SWCNHs in a polymer solution.

Due to this procedure the obtained polymer suspensions with carbon nanohorns are stable within 24 h, as shown in Fig. 7. The absorbance of SU samples measured for the initial samples (immediately after dispersion) and after 24 h differs 10% only. For the samples SU10 the absorbance values both immediately after dispersion process and 24 h later remain at the same level. Summarising, the stability of SWCNHs contained PAN solution after 24 h is maintained.

The results of the mechanical tests for selected PAN-based nanocomposite samples are summarized in Table 2. The differences between nanocomposites are significant depending on the preparation of polymer suspensions, i.e., prepared after gradual sonication of SWCNHs in the DMF

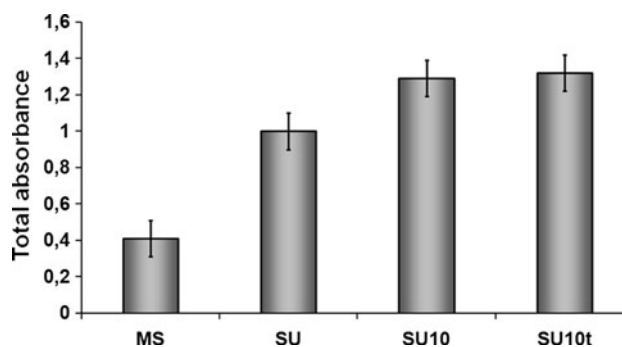**Fig. 5** Pure PAN solution and PAN suspension containing SWCNH after optimisation process

Fig. 6 IR absorbance of PAN suspensions containing carbon nanotubes

and PAN suspensions (SU10) and after sonification directly in the PAN solution (MS). The presence of large size agglomerated carbon particles in nanocomposites (MS) matrix causes a distinct fall in the strength (almost 30%) and 35% in tensile modulus in comparison with the pure polymer samples. Mechanical properties of the samples containing 0.5 wt% (SU10) nanohorns obtained from optimally prepared suspension are considerably higher than
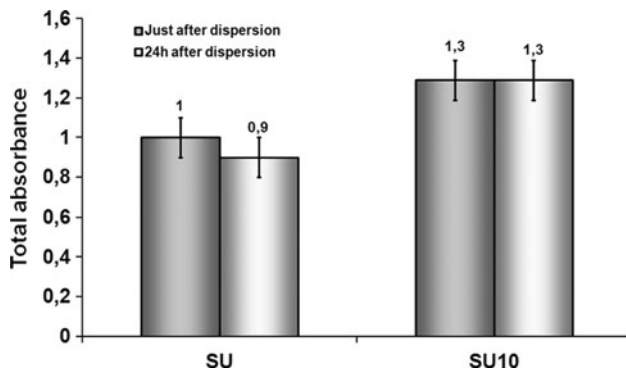
Fig. 7 Absorbance measured for initial solution containing dispersed SWCNHs and after 24 h

those obtained for pure polymer samples and for the samples, which were sonicated only (MS).

Using the third dispersion procedure two additional samples differing in SWCNHs amount were prepared. The mechanical properties of the resulting samples are gathered in Table 3. By comparing the shapes of load–strain curves some new information on dispersion effect can be achieved. Figure 8 illustrates these curves for the pure polymer (PAN) and nanocomposites manufactured from the suspensions containing a different amount of nanohorns. Two parts for each curve can be distinguished; initial linear and nonlinear one. There is a little change in the initial linear part of the slope representing the tensile modulus of a sample. This indicates that the effect of nanoparticles introduced into the polymer matrix on the tensile modulus is not significant (see Table 3). The PAN material is a linear polymer containing strong nitrile polar groups and ternary hydrogen bonds involved in creation of strong cross-linking bonds between the polymer chains. It is a well-known fact that weakening these bonds (e.g., by heating, oxidation) leads to significant lowering in the tensile modulus of the PAN polymer. In our experiments such an effect is not observed. It seems reasonable to conclude, therefore, that the interaction of carbon nanoparticles with the polymer is a physical in nature. Their influence on the mechanical properties is similar to that observed for composites reinforced with neutral small particulates. Depending on the concentration of dispersed nanohorns and their size (the smallest size corresponds to *dahlia flower-like* nanoparticle) the mechanical properties

Table 2 Mechanical properties of pure PAN sample and nanocomposite samples (MS and SU10)

Samples	Tensile strength Rm (MPa)	Young's modulus E (GPa)
PAN	61.5 ± 7.0	2.6 ± 0.4
MS	44.4 ± 7.4	1.7 ± 0.3
SU10	80.4 ± 5.3	3.0 ± 0.6

are changed. However, variations in mechanical properties (strength, modulus, Table 3) are much smaller than those obtained by the other authors for the PAN polymer reinforced with MWCNTs [13, 35] On the contrary, much more significant changes are accompanied by the changes in nonlinear part of the curves. The transition point of these functions from linear to nonlinear part takes place at different level of tensile loads, depending on the type of suspension. The total strain to failure for the SU10a sample is almost three times higher (mean value 21.0%) as compared to the pure PAN sample. The linear part of the strain is almost the same, irrespectively of the type of nanocomposite. It may suggest that carbon nanohorns are better dispersed in the PAN matrix suspension prepared in such conditions (SU10a), and after solidification the nanocomposite displays an optimum supramolecular structure. During the tensile test such a nanocomposite in its nonlinear phase, round in shape and small nanohorn aggregates are located between the polymer chains facilitating their reorientation and straightening.
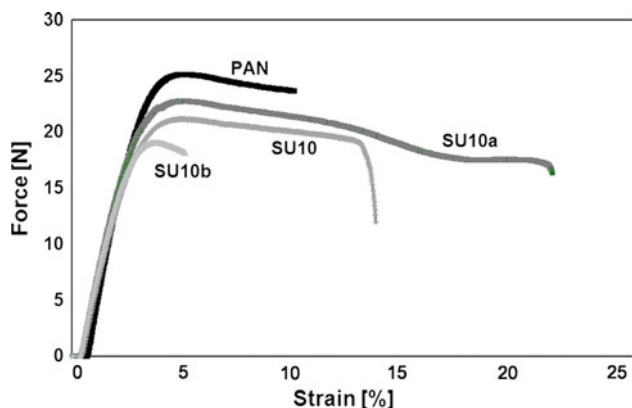
A decrease in the mechanical properties of the samples containing a higher amount of SWCNH (3 wt%) is probably caused by a secondary agglomeration of nanohorns that form bigger nanoparticles. It is confirmed by the mean size of agglomerates and the values of total strain to fracture (Table 3). The 3% addition of nanohorns significantly affects the deformation to failure, decreasing maximum strain-to-failure to the level of three times lower than that obtained for the pure polymer, indicating that the nanocomposite became brittle.

As expected the suspensions containing additionally surfactant allowed for further enhancement of mechanical properties of the nanocomposites (SU10ta) (Table 4). Two nanocomposites with the same concentration of nanohorns were compared. For the samples manufactured with surfactant about 10% increase in the tensile modulus and no significant change in the tensile strength were noted. Although these experiments were made under constant processing variables (sonication time, power), the results showed that typical dispersion techniques applied to this particular carbon nanoform do not permit to separate its as-fabricated aggregated *dahlia flowers* form to a single nanohorn. The lowest values of the dispersed carbon nanoparticles (50–250 nm) consisted of several single nanohorns are close to those observed by TEM (30–120 nm).

The pure PAN and nanocomposites before (MS) and after (SU10) dispersion process of SWCNH were characterized using XRD technique. The XRD diffractogram for the PAN samples exhibits one broad peak at $2\theta = 17.1°$, which can be ascribed to the (100) planes in the PAN crystallite structure. A strong, narrow peak at $2\theta = 26.5°$ for the (002) planes in nanocomposites corresponds to the presence of SWCNH (Fig. 9a).

Table 3 Mechanical properties of pure PAN sample and nanocomposite samples containing different concentration of SWCNH (SU10, SU10a and SU10b)

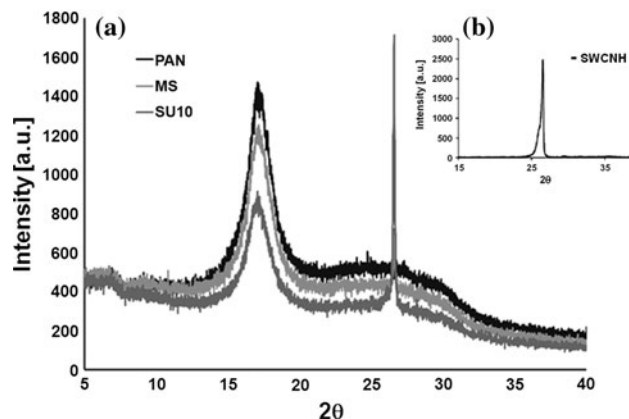| Samples	Tensile strength RM (MPa)	Young's modulus E (GPa)	Strain to failure ε (%)	Mean value of SWCNH agglomerates (nm)
PAN	61.5 ± 7.0	2.6 ± 0.4	7.2 ± 1.0	–
SU10 (0.5 wt% of SWCNH)	80.4 ± 5.3	3.0 ± 0.6	13.2 ± 4.2	142.0 ± 1.5
SU10a (1 wt% of SWCNH)	84.4 ± 7.7	3.1 ± 0.3	21.0 ± 6.4	150.0 ± 2.5
SU10b (3 wt% of SWCNH)	65.9 ± 6.6	2.9 ± 0.3	2.4 ± 0.5	392.0 ± 3.5

Fig. 8 The tensile force–strain relationship of the pure polymer (PAN) and nanocomposites

Fig. 9 X-ray diffraction patterns of pure PAN, nanocomposites (MS and SU10) (*a*) and SWCNHs (*b*)

The SWCNHs aggregate due to van der Waals interaction creates double-layered region, where X-rays are scattered [3]. The XRD diffractogram of SWCNHs is shown in Fig. 9b. The calculated apparent crystallite sizes for the pure PAN samples and modified MS and SU10 nanocomposites are gathered in Table 5.

As it results from this analysis the range of crystalline ordering in nanocomposites obtained from the suspension after gradual dispersion (SU10) is higher in comparison with the pure PAN and MS samples. The PAN polymer displays a semi-crystalline structure containing amorphous regions that under appropriate conditions can be transformed into a crystalline molecular structure. The SWCNHs possessing a high surface energy may play a role of nucleation sites promoting crystallization of the polymer chains [43, 44]. It is also likely that the acrylonitrile monomers may be adsorbed on the surface of the SWCNHs and during solidification process in the amorphous regions of the PAN polymer the cross-linked structure is formed [44]. Due to a higher

dispersion, level of SWCNHs such an effect is stronger in the polymer (SU10) than that in MS nanocomposites.

These observations are consistent with DSC analysis of the pure PAN and nanocomposites before and after dispersion of carbon nanotubes (Fig. 10).

The values of the initiation temperature (T_s) and maximum exothermic temperature (T_e) determined from DSC exotherms are shown in Table 6.

The nanocomposites (SU10) manufactured from the PAN suspension with well-dispersed SWCNHs show higher values both for T_s and T_e than those found for the pure PAN and MS nanocomposites without an appropriate dispersion. This may be attributed to a better crystallinity of the PAN matrix in SU10 samples resulting in inhibition of the cyclization process by nitrile groups in comparison with the PAN and MS samples.

Electrical and thermal properties were tested for selected samples obtained following gradual dispersion of SWCNHs in the PAN suspension. Electrical resistivity of

Table 4 Mechanical properties of pure PAN samples and nanocomposite samples containing 1 wt% of SWCNH with (SU10ta) and without (SU10a) surfactant

Samples	Tensile strength RM (MPa)	Young's modulus E (GPa)
PAN	61.5 ± 7.0	2.6 ± 0.4
SU10a	84.4 ± 7.7	3.1 ± 0.3
SU10ta	87.8 ± 6.3	3.4 ± 0.5

Table 5 XRD data for PAN and PAN/SWCNH nanocomposites

	Angle 2θ (°)	L_c (Å)
PAN	17.1	49.3
MS	17.1	46.5
SU10	17.1	55.0

nanocomposites containing 1 wt% (SU10a) and 3 wt% (SU10b) of SWCNHs is gathered in Table 7.

The electrical resistivity for pure PAN samples is undetectable and is an order of 10^4 kΩ m [45], whereas for nanocomposites (SU10a) this value is $\rho = 6.9 \pm 0.8$ kΩ m. The pure PAN matrix is a typical insulator, and conducting properties can be reached when conducting filler constitutes a continuous component in the nonconductive matrix. Due to superior electrical properties of carbon nanotubes they can be used as electrical conductors. Electrical conductivity of this nanocomposite depends on through-going chain mechanism between conductive nanohorns creating a *dahlia flower-like* nanoparticles. The carbon nanohorns should create the conductive continuous paths and such a phenomenon proceeds as the percolation threshold is achieved. The results gathered in Table 7 testify that 1 wt% amount of SWCNHs is able to form the electrical conductivity mesh in the PAN matrix. Although such a mechanism easily explains electrical behaviour of the PAN-based nanocomposite samples an another possible mechanism cannot be excluded, namely it was found that there is also conducting phenomenon even if the gaps between conductive fillers in the polymer matrix exist [46]. The conduction increase can result from electron charge transfer via hopping or tunnelling mechanism in the conductive PAN. It is apparent from our XRD data that a better crystalline ordering of PAN structure is observed for nanocomposite samples after an effective dispersion of carbon nanohorns. It can be assumed that such a phase is
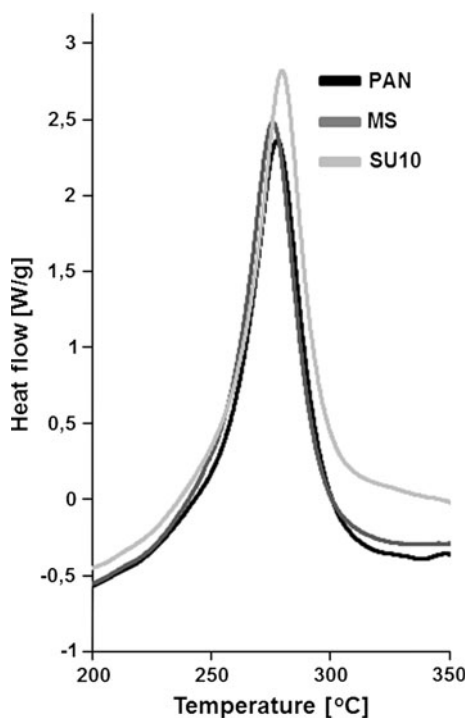
Table 6 DSC date for pure PAN and nanocomposites (MS and SU10)

Samples	T_s (°C)	T_e (°C)
PAN	255	278
MS	254	277
SU10	259	280

Table 7 Electrical resistivity and thermal conductivity of pure PAN samples and nanocomposites containing SWCNH

Samples	Electrical resistivity (kΩ m)	Thermal conductivity (W/mK)
PAN	10^4 [45]	0.27 ± 0.05
MS	>330.0	–
SU10a	6.9 ± 0.8	0.44 ± 0.09
SU10b	4.4 ± 0.5	–

formed in the proximity of conductive carbon nanoparticles. Different articles indicate that the electrical conduction of polymer nanocomposites containing carbon nanoparticles may be attainable even at a distinctly lower concentration of CNTs (0.001 wt%), and this effect depends on the types of CNTs, polymeric matrices and dispersions degree of nanocarbons [47–53]. With increasing concentration of SWCNHs in the PAN-based nanocomposites the electrical resistivity decreases and for nanocomposites containing 3 wt% of SWCNHs (SU10b) the value of resistivity is 31% lower in comparison with samples containing 1 wt% of SWCNHs (SU10a).

The thermal conductivity was measured for the pure PAN polymer and selected nanocomposites after optimization of the dispersion process of SWCNH (SU10a).

As shown in Table 7, the conductivity of nanocomposites (SU10a) is almost 63% higher as compared to the pure polymer samples. The presence of a very small amount of well-dispersed carbon nanohorns in the PAN suspension contributes distinctly to the overall conductivity of the PAN-based nanocomposites. It worth to note that the nanohorn-contained particles were uniformly distributed in the polymer matrix and the resulting nanocomposites constituted isotropic laminates. The lack of matrix–nanohorn contacts would be expected to reduce the conductivity along the sample length. The observed increase in conductivity suggests, however, that the heat is also transferred from the polymer matrix to nanohorn-based aggregates, which indicates that the matrix–carbon domains interaction is strong. Typical single walled carbon nanotubes are known to have a high thermal conductivity, the theoretical value of which is about 6600 W/mK [54]. The impact of the carbon nanohorns on thermal conductivity of polymer nanocomposites has already been confirmed in literature

Fig. 10 DSC curves for pure PAN and nanocomposites SU and SU10

[55, 56]. Moreover, as it was found from XRD measurements the presence of SWCNHs the polymer matrix improves its structural ordering, which also contributes to thermal conduction and ensures a better heat transfer throughout the sample.

Conclusions

The PAN-based nanocomposites modified with SWCNHs in the form of thin films have been obtained from polymer suspensions prepared in different ways. Effect of dispersion degree of carbon nanoparticles related to mechanical and physical behaviour was analysed. Direct incorporation of SWCNHs without their dispersion in a PAN solution revealed the presence of large agglomerates. Such agglomerates were found both in the polymer solution and in the solidified samples in the form of film. After sonication in optimum conditions, a homogeneous PAN solution was prepared. The best homogeneity of the suspension containing carbon nanohorns was achieved for nanocomposites by the combined assistance of ultrasonication and surfactant adsorption. The presence of well-dispersed nanohorn particles in the PAN matrices promotes the increase of the strain to failure of nanocomposites in nonlinear phase under tensile test. The presence of SWCNHs aggregates in polymer samples after optimization of the dispersion process augments electrical and thermal conductivities of nanocomposites. The lowest values of carbon aggregates (50–250 nm) observed in the PAN suspension after disintegration procedure are in fairly good agreement with the mean size of a *dahlia flower-like* structure of nanohorns particle.

References

1. Battiston S, Bolzan M, Fiameni S, Gerbasi R, Meneghetti M, Miorin E, Mortalo C, Pagura C (2009) Carbon 47:1321
2. Dresselhaus MS, Dresselhaus G, Avouris Ph (2001) Carbon nanotubes synthesis structure properties and applications. Springer, Berlin
3. Bandow S, Kokai F, Takahashi K, Yudasaka M, Qin LC, Iijima S (2000) Chem Phys Lett 321:514
4. Iijima S, Yudasaka M, Yamada R, Bandow S, Suenaga K, Kokai F, Takahashi K (1999) Chem Phys Lett 309:165
5. Tanaka A, Umeda K, Yudasaka M, Suzuki M, Ohana T, Yumura M, Iijima S (2005) Tribol Lett 19:135
6. Tsuji H, Kawashima Y, Takikawa H, Tanaka S (2007) Polymer 48:4213
7. Cato AD, Edie DD (2003) Carbon 41:1411
8. Wangxi Z, Jie L, Gang W (2003) Carbon 41:2805
9. Rahaman MSA, Ismail AF, Mustafa A (2007) Polym Degrad Stab 92:1421
10. Wan LS, Xu ZK, Huang XJ, Che AF, Wang ZG (2006) J Membr Sci 277:157
11. Min HS, Ko JM, Kim DW (2003) J Power Sources 119:469
12. Min BG, Sreekumar TV, Uchida T, Kumar S (2005) Carbon 43:599
13. Chae HG, Sreekumer TV, Uchida T, Kumar S (2005) Polymer 46:10925
14. Jagannathan S, Liu T, Kumar S (2010) Compos Sci Technol 70:593
15. Fraczek-Szczypta A, Bogun M, Blazewicz S (2009) J Mater Sci 44:4721. doi:10.1007/s10853-009-3730-2
16. Murata K, Kaneko K, Kokai F, Takahashi K, Yudasaka M, Iijima S (2000) Chem Phys Lett 331:14
17. Murata K, Kaneko K, Steele W, Kokai F, Takahashi K, Kasuya D, Hirahar K, Yudasaka M, Iijima S (2001) J Phys Chem B 105:10210
18. Jorio A, Dresselhaus G, Dresselhaus MS (2008) Carbon nanotubes, Topics Appl Physics, vol 111. Springer-Verlag, Berlin Heidelberg, pp 605–629
19. Ham HT, Choi YS, Chung IJ (2005) J Colloid Interface Sci 286:216
20. Tucknott R, Yaliraki SN (2002) Chem Phys 281:455
21. Girifalco LA, Hodak M, Lee RS (2000) Phys Rev B 62:13104
22. Coleman JN, Khan U, Blau WJ, Gunko YK (2006) Carbon 44:1624
23. Xie XL, Mai YW, Zhou XP (2005) Mat Sci Eng R 49:89
24. Sreekumar TV, Chandra L, Srivastava A, Kumar S (2007) Carbon 45:1105
25. Owens FJ (2005) Mat Lett 59:3720
26. Vaisman L, Wagner HD, Marom G (2006) Adv Colloid Interface Sci 128–130:37
27. Strano MS, Moore VC, Miller MK, Allen MJ, Haroz EH, Kittrell C, Hauge RH, Smalley RE (2003) J Nanosci Nanotechnol 3:81
28. Bose S, Bhattacharyya AR, Kulkarni AR, Pötschke P (2009) Compos Sci Technol 69:365
29. Bose S, Khare RA, Moldenaers P (2010) Polymer 51:975
30. Mikolajczyk T, Rabiej S, Szparaga G, Bogun M, Fraczek-Szczypta A, Blazewicz S (2009) Fibres Text East Eur 17:13
31. Mikolajczyk T, Szparaga G, Bogun M, Fraczek-Szczypta A, Blazewicz S (2010) J Appl Polym Sci 115:3628
32. Fraczek-Szczypta A (2009) Doctor's thesis, Krakow
33. Fraczek A, Blazewicz S (2009) J Phys Conf Ser 146:012005-1
34. Fraczek A, Blazewicz S, Bogun M, Szparaga G (2007) Karbo 4:201
35. Guo H, Sreekumar TV, Liu T, Minus M, Kumar S (2005) Polymer 46:3001
36. Rastogi R, Kaushal R, Tripathi SK, Sharma AL, Kaur I, Bharadwaj LM (2008) J Colloid Interface Sci 328:421
37. Velasco-Santos C, Martınez-Hernandez AL, Fisher F, Ruoff R, Castano VM (2003) J Phys D Appl Phys 36:1423
38. Kataura H, Kumazawa Y, Maniwa Y, Umezub I, Suzuki S, Ohtsuka Y, Achiba Y (1999) Synth Met 103:2555
39. Murakami Y, Einarsson E, Edamura T, Maruyama S (2005) Phys Rev Lett 94:087402-1
40. Kazaoui S, Minami N, Kataura H, Achiba Y (2001) Synth Met 121:1201
41. Lian Y, Maeda Y, Wakahara T, Nakahodo T, Akasaka T, Kazaoui S, Minami N, Shimizu T, Tokumoto H (2005) Carbon 43:2750
42. Kang B, Dai Y, Chang S, Chen D (2008) Carbon 46:974

43. Wu D, Wu L, Zhou W, Zhang M, Yang T (2010) Polym Eng Sci 50:1721
44. Zhang H, Xu L, Yang F, Geng L (2010) Carbon 48:688
45. Fan JH, Wan MX, Zhu DB (1997) Polym Bull 1:22
46. Ghosh P, Chakrabarti A (2000) Eur Polym J 36:1043
47. Thostenson ET, Chou TW (2006) Carbon 44:3022
48. Sandler JKW, Kirk JE, Kinloch IA, Shaffer MSP, Windle AH (2003) Polymer 44:5893
49. Bryning MB, Islam MF, Kikkawa JM, Yody AG (2005) Adv Mater 17:1186
50. Grunlan JC, Mehrabi AR, Bannon MV, Bahr JL (2004) Adv Mater 16:150
51. Zhang Q, Rastogi S, Chen D, Lippits D, Lemstra PJ (2006) Carbon 44:778
52. Anoop Anand K, Agarwal US, Anuya N, Rani J (2007) Eur Polym J 43:2279
53. Li C, Thostenson ET, Chou TW (2008) Compos Sci Technol 68:1227
54. Berber S, Kwon YK, Tomanek D (2000) Phys Rev Lett 84:4613
55. Hong WT, Tai NH (2008) Diam Relat Mater 17:1577
56. Song YS, Youn JR (2006) Carbon 44:710